

Birefringence Properties and Surface Relief Grating Formation on Methacrylate Polymers with Photochromic Side Chains

S. Ahmadi-Kandjani^a, P. Tajalli^c, H. Khoshsima^a, R. Barille^c, J. –M. Nunzi^d, S. Kucharski^e, and H. Tajalli^{a,b}

^aResearch Institute for Applied Physics and Astronomy, University of Tabriz, Iran

^bFaculty of Physics, University of Tabriz, Iran

^cLaboratoire POMA, Université d'Angers, Angers, France

^dDepartment of Chemistry, Chernoff Hall, Queen's University, Canada

^eWroclaw University of Technology, Faculty of Chemistry, Department of Polymer Engineering and Technology, Wroclaw, Poland.

Abstract- We have studied light-induced birefringence (LIB) and surface relief grating (SRG) formation in the series of methacrylate polymers. The effect of material structure such as length of photochromic side chain, glass transition temperature and molecular structure of azo units on LIB and SRG are studied. The optical formation of self-induced SRG on films of these materials is also presented.

KEYWORDS: Surface relief grating, light-induced birefringence, methacrylate polymers, photoisomerization

I. INTRODUCTION

Surface relief gratings (SRG) manufactured by the holography technique in azo-polymers have recently found wide utilisation and their areas of application are constantly widening. SRG can be used as couplers (wave-guide input-output elements), filters, polarization separators, liquid crystal orientation, holographic data storage, waveguides, etc. [1-5].

The main interest of azo-polymers for the SRG formation is due to their dichroic and birefringent properties when they are illuminated by a polarized light. This behavior is because of a reversible "trans-cis" photoisomerization with respect to the N=N double bond and redistribution in the orientation of the azo dye molecules (perpendicular to the polarization direction of light) [6].

Following to this photoisomerization cycles, the large-scale mass transport of the azo polymer chains occurs by moving from bright to dark region of interference pattern, which results modulation of surface in a reversible way. Several mechanisms by various research groups have been proposed to explain SRG formation in azo-polymers [7-11].

In order to understand the mechanism of SRG formation and to design high-performance SRG- forming materials (photoprocessability and photoresponse behaviour), it is necessary to elucidate the relationship between molecular structure and SRG formation.

Different classes of azobenzene polymers including polymeric matrices, such as epoxy, polyacrylates, liquid-crystalline polyesters, azo hybrid gel films, polyurea and conjugated polymers such as polydiacetylene and polyacetylene have been used for SRG formation [12–18]. These materials can be in the form of both side chain as well as main chain azo-polymers. The recorded SRGs are stable below the glass transition temperature T_g , and can be erased optically. SRGs are strongly depended on the polarization and the energy of the recording beams.

Spontaneous hexagonal structure has been formed on the surface of an azo-polymer by illuminating the polymer film with a linearly polarized laser beam. The elongation direction

of the hexagons depends on the polarization direction of the laser beam [19].

We have recently demonstrated that spontaneous periodic SRGs can form on the surface of low-T_g azo-polymers. The wave vector of formed gratings is parallel to the polarization direction of writing beam and multistate polarization storage can achieve in these materials [20].

In this experimental work we presented the light-induced birefringence (LIB), two beams and self induced SRG formation on the methylacrylate azo-polymer films. Our goal was to investigate the influence of material structures on these optical effects.

II. EXPERIMENTS, RESULTS AND DISCUSSIONS

A. Materials

In this work methylacrylate polymers with photochromic side chains, derivatives of azobenzene containing heterocyclic sulfonamide moieties, were used. The maximum absorbance wavelength and dipole moments of side chain units are presented in Table 1. Dipole moments have been calculated by Gaussian RHF/3-21g for isolated molecule [21]. The structural formulas are given in Fig. 1.

Table 1: Wavelength of maximum absorbance λ_{\max} and dipole moment μ of chromophores

| Monomer | λ_{\max} (nm) | $\mu / 10^{-30}$ (C m) trans - cis | |
|---------|-----------------------|---------------------------------------|-------|
| 1I | 440 | 34.10 | 27.84 |
| 2I | 446 | 35.29 | 17.53 |
| 3I | 450 | 34.65 | 13.28 |
| 2M | 454 | 29.31 | 14.14 |

The monomers of the methylacrylate type contained aliphatic spacers (1,2,3I) of different length between chromophoric and methylacrylic groups. These monomers were copolymerized with butyl 2-methylacrylate (MB) and 2-ethylhexyl acrylate (AI) to get copolymers containing various chromophoric units such as MB1I, MB2I, MB3I, AI2I and AI2M. Preparation of these polymers is described elsewhere [22]. Glass transition temperature, wavelength of maximum

absorbance and absorbance at the working wavelength of the polymers have been shown in Table 2.

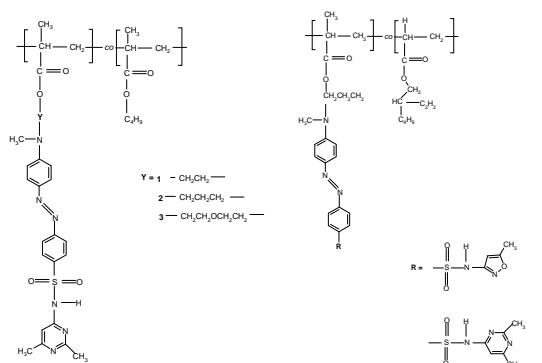


Fig. 1 Chemical structures of the materials. MBYI (left) with different spacers Y(=1, 2, 3) and AI2R (right) with different end group R(=I, M).

Table 2: Glass transition temperature T_g, wavelength of maximum absorbance λ_{\max} and absorbance at 488 nm of azo-polymers.

| Polymer | T _g (°C) | λ_{\max} (nm) | A ₄₈₈ |
|---------|---------------------|-----------------------|------------------|
| MB1I | 86.2 | 433 | 1.3 |
| MB2I | 71.1 | 438 | 1.33 |
| MB3I | 71.5 | 435 | 1.55 |
| AI2I | 57.5 | 435 | 1.13 |
| AI2M | 53 | 445 | 1.42 |

Thin films of polymers on glass substrates were prepared by spin-coating 50 mg/ml polymers solutions in TetrahydroFuranne (THF) solvent. Using a profiler, Dektak-6M Stylus Profiler, thickness of the thin films were measured about $\sim 0.45 \mu\text{m}$. Fig. 2 shows the absorbance of the polymer films. The $\lambda = 488$ nm laser line of a continuous argon ion laser was used as a pump beam for light-induced birefringence and grating formation in thin films.

B. Light-induced birefringence experiments

The experimental setup for measuring light-induced birefringence is shown in Fig. 3.

An Ar ion laser (488 nm) is used as pump beam inside the absorption band of polymers, and a He-Ne laser (633 nm) is used as a probe beam. The transmission of the He-Ne laser through the film placed between crossed polarizers is recorded by a photodiode as a function of time after irradiation with the

pump beam polarization set at 45° angle with respect to the probe beam polarization. The pump induces optical anisotropy in the film.

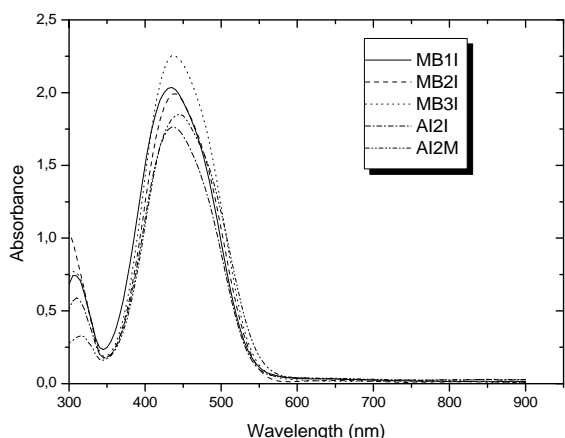


Fig. 2 The UV-vis spectra of materials

Birefringence modulus Δn is given by:

$$\Delta n = \frac{\lambda_o}{\pi d} \arcsin \left(\sqrt{\frac{I(t)}{I_o}} \right), \quad (1)$$

where λ_o , d , $I(t)$ and I_o are wavelength of the probe beam, thickness of the film, intensity of transmitted and incident probe beam, respectively.

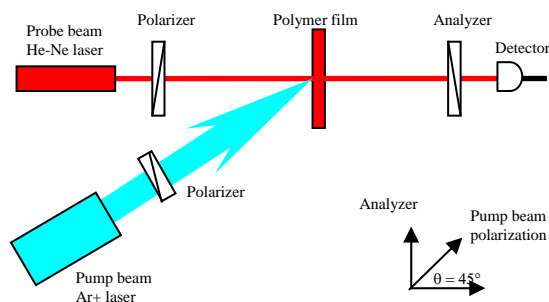


Fig. 3 The experimental setup for measurements of light-induced birefringence. The polarization direction of pump beam is in 45° with respect to polarizer and analyzer direction of probe beam.

Figure 4 shows a typical birefringence excitation - relaxation sequence. The birefringence signal increase rapidly and reaches saturation after the pump beam is turned on at point A. It decreases and reaches to a constant value that will be kept constant for a long time in the dark after the writing beam is then turned off at point B. The dynamics of birefringence decay, in the

absence of pump beam, have been studied by biexponential function for the assumption of fast and slow decays [23].

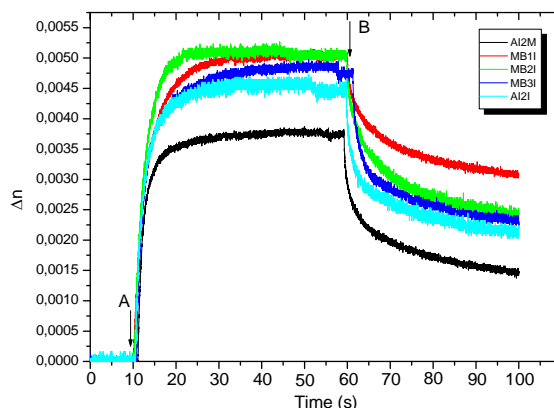


Fig. 4 Birefringence Δn in polymer films as a function of time: (A) The pump (writing) beam is turned on. (B) The writing beam is turned off. Pump beam intensity is 100 mW/cm². The birefringence is measured by a He-Ne laser at 632.8 nm.

The biexponential function is

$$\Delta n(t) = A + B \exp(-\tau_1 t) + C \exp(-\tau_2 t) \quad (2)$$

where A is the birefringence conserved for a long times, τ_1 , τ_2 are the relaxation rates with amplitudes of B and C respectively. The normalized parameters obtained by fitting equation 2 to the experimental results summarized in Table 3. The results show that for low-Tg azo-polymers, saturated value of Δn_s and stable values of the photoinduced birefringence A decrease with the decrease of Tg. The relaxation rates, τ_1 and τ_2 of the photoinduced birefringence increase with the decrease of Tg.

Table 3: Fitting parameters A , B and C , relaxation rates, τ_1 and τ_2 and saturated value of photoinduced birefringence Δn_s

| Polymer | A | B | C | τ_1 (1/s) | τ_2 (1/s) | Δn_s |
|---------|------|-------|-------|----------------|----------------|--------------|
| MB1I | 0.66 | 0.279 | 0.275 | 0.446 | 0.053 | 0.0051 |
| MB2I | 0.67 | 0.307 | 0.310 | 0.476 | 0.068 | 0.0052 |
| MB3I | 0.63 | 0.374 | 0.268 | 0.431 | 0.032 | 0.0048 |
| AI2I | 0.68 | 0.354 | 0.276 | 0.630 | 0.045 | 0.0045 |
| AI2M | 0.60 | 0.330 | 0.319 | 0.900 | 0.058 | 0.0038 |

The process is interpreted as trans-cis-trans isomerization and reorientation of the azobenzene derivatives. Many write - erase cycles can be achieved without significant

degradation. This shows that polymer films in question can be used for reversible optical storage purposes.

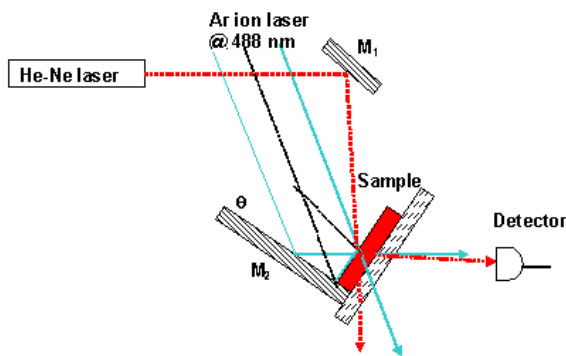


Fig. 5 Schematic diagram for the measurement of diffraction efficiency of the SRG in polymeric films. M_1 and M_2 are mirrors. The angle θ is 10° .

C. SRG formation experiments

We checked the capability of polymers to make SRG. The gratings were optically inscribed onto the films with a single laser beam partly split by a mirror and reflected onto the film surface using the Lloyd mirror setup shown in Fig. 5.

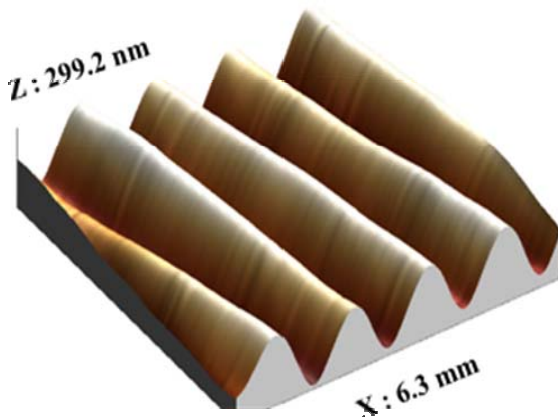


Fig. 6 AFM profile of the formed SRG on the azo-polymer film.

The 488 nm line from an argon laser expanded to a diameter of 8 mm was used for writing. Grating inscription was monitored by measuring the growth of the first-order diffracted beam over time with a 5 mW, 633 nm He-Ne laser probe, in the transparency region of the material. We used orthogonally polarized beam configuration (right and left circular) for interfering beams. The probe beam was p-polarized. Efficiencies were measured as the percentage of first-order

diffracted beam intensity to the transmitted light. The angle (θ), as shown in Fig. 5, is maintained at $\sim 10^\circ$ to obtain a grating periodicity of $\Lambda \sim 1.4 \mu\text{m}$. The surface morphology of the samples was imaged with a Pico SPM from Molecular Imaging. Atomic force microscopy was performed in contact mode with a maximum scanning area of $6.5 \times 6.5 \mu\text{m}$ (Fig. 6).

The diffraction efficiencies for polymers with different spacers (MB1I, MB2I, and MB3I) were presented in Fig. 7. By increasing the length of spacer, the diffraction efficiency was decreased.

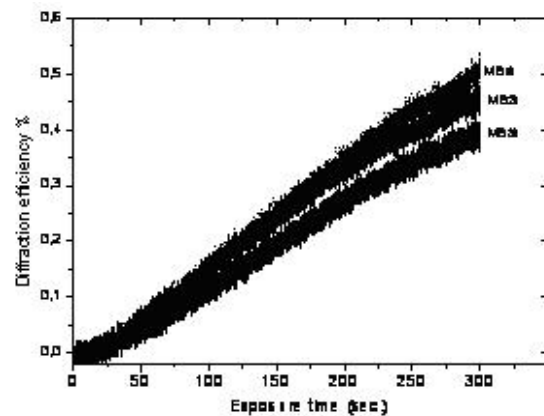


Fig. 7 Diffraction efficiencies of SRG formed on the surface of azo polymer films with different chromophore length as a function of time.

Figure 8 shows diffraction efficiencies for two different azo-polymers with the same azo side chain (MB2I and AI2I). The result shows that for polymer with higher glass transition temperature (T_g), the diffraction efficiency is lower because of difference in diffusion coefficient [24].

Figure 9 shows the diffraction efficiency for polymers with different azo side chain (AI2I and AI2M). However, as the T_g value of AI2I is higher than AI2M, the diffraction efficiency is higher for AI2I as compared with AI2M. It can be explain by the difference in the dipole moment of azo unit, the dipole moment of 2M is less than 2I and efficiency of light-matter interactions is lower.

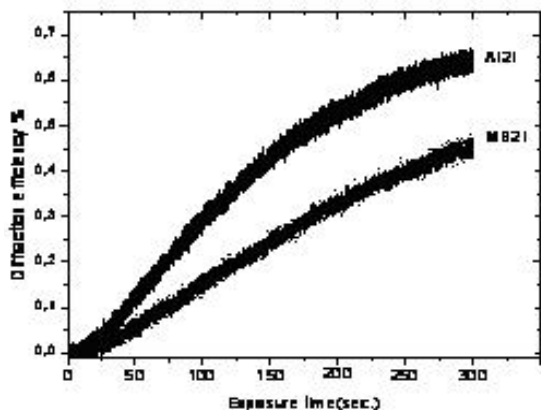


Fig. 8 Diffraction efficiencies of SRG formed on the surface of azo polymer films with different Tg as a function of time.

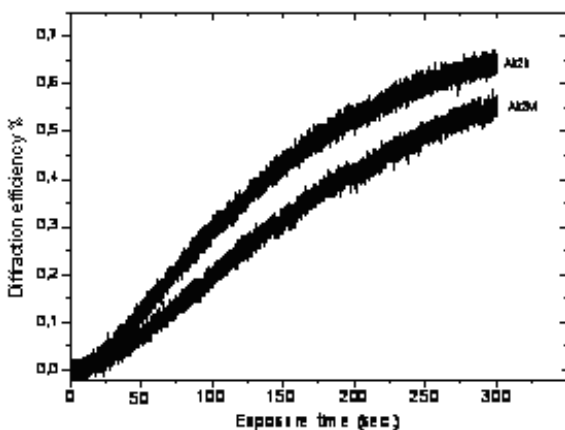


Fig. 9 Diffraction efficiencies of SRG formed on the surface of azo polymer films with different chromophores as a function of time.

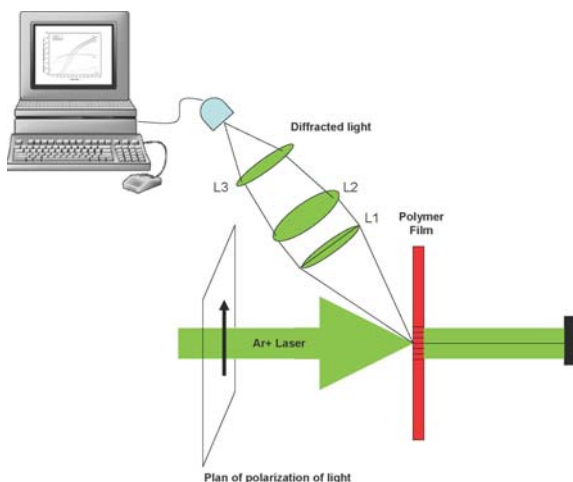


Fig. 10 Experimental setup for printing the self-induced SRGs.

D. Self-induced SRG formation

Our experimental setups are depicted in Fig. 10. Incoming light intensity is controlled by the power supply. Polarization direction of the laser beam is varied using a half-wave

plate. Sample is set perpendicular to the incident laser beam. The size of the collimated laser beam impinging onto the polymer sample is controlled with a Kepler-type afocal system. Sample is irradiated with different polarizations using different laser beam intensities with a beam size of 4 mm diameter at $1/e^2$. In order to monitor the formation of photoinduced SRG, the intensity of writing beam backward diffraction was measured by a photodiode.

Figure 11 presents the diffracted beam intensity as a function of time for different materials. The intensity rises over several tens of minutes and finally saturated. The rate of growth and maximum value of diffracted beam intensity depend on the material structure.

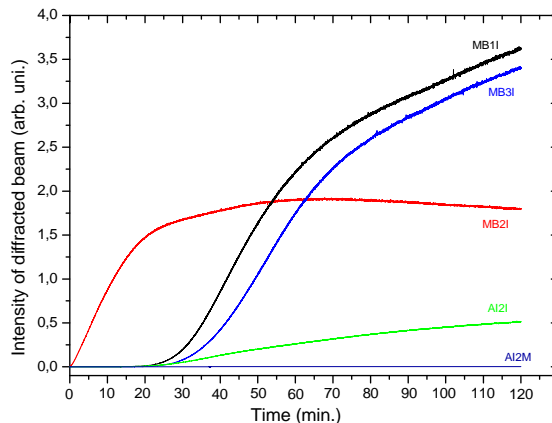


Fig. 11 Diffracted beam intensity as a function of time for different materials. The intensity of writing beam is 450 mW/cm^2 at 488 nm.

Figure 12 shows the influence of writing beam power on the grating formation process. In the case of MB2I (Fig. 12.a) for low powers, diffracted beam intensity rises and then saturated but for higher intensities, it increases, reaches to a maximum and then drops to some constant value. We think that the relaxation of diffracted beam intensity can be due to the reorientation of azo group or deformation of SRG [25]. Typically Fig. 12.b shows the influence of writing beam power for the other materials that used in this study (for example MB3I). The results show that by increasing the power of writing beam, the rate of growth is increased (Fig. 12.a-b). Figure 13 shows the typical AFM image of self-induced SRGs, the pitch of grating is around 800 nm

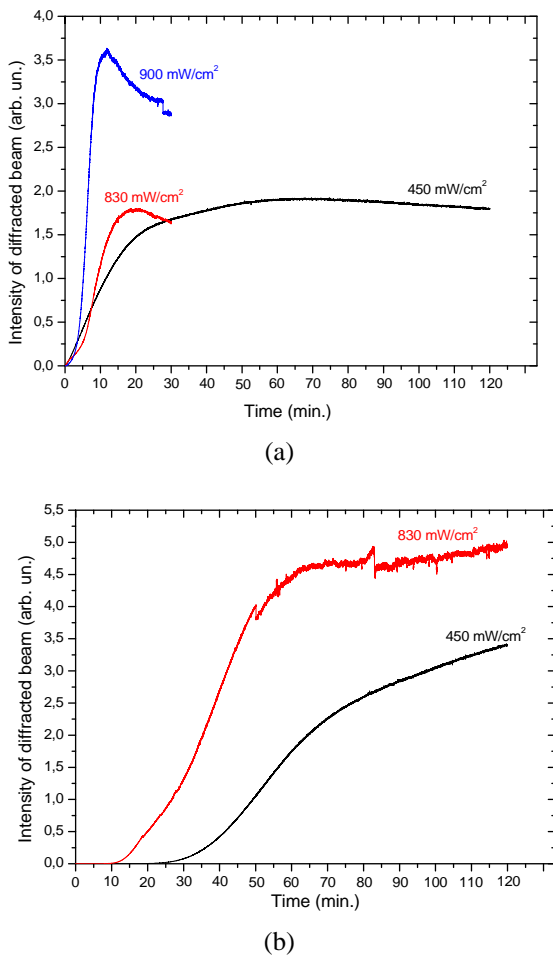


Fig. 12 Diffracted beam intensity for different power of writing beam in the case of MB2I and MB3I respectively.

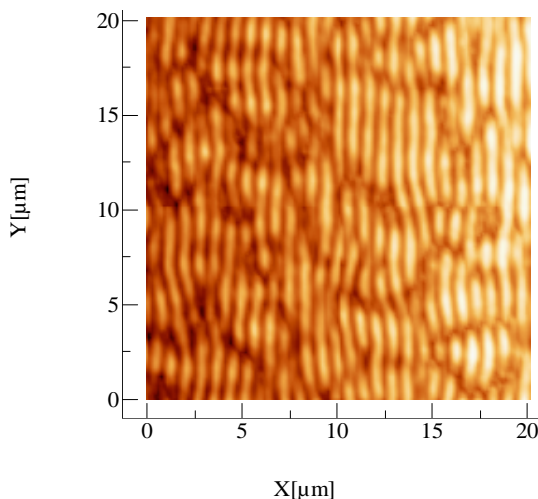


Fig. 13 Typical AFM image of self-induced SRGs.

III. CONCLUSION

Five novel azo-polymers were studied. Light-induced birefringence studies showed that its saturation value, relaxation rates and stability depend on T_g of materials. Surface relief

gratings and self-induced SRGs were inscribed on these azo-polymers. SRG formation on azo-polymer films and its diffraction efficiencies depend on both polymer main chain and chromophore structure. The results showed that these materials are suitable for all applications related to SRGs. The self-induced SRGs will provide for these polymers some new applications.

ACKNOWLEDGMENT

This work has been supported partially by Center for International Research and Collaboration (ISMO) and French Embassy in Tehran and by the research grant of the University of Tabriz.

REFERENCES

- [1] J. Paterson, A. Natansohn, P. Rochon, C. L. Callender, and L. Robitaille, "Optically inscribed surface relief diffraction gratings on azobenzene-containing polymers for coupling light into slab waveguides," *Appl. Phys. Lett.*, Vol. 69, pp. 3318-3320, 1996.
- [2] P. Rochon, A. Natansohn, C. L. Callender, and L. Robitaille, "Guided mode resonance filters using polymer films," *Appl. Phys. Lett.*, Vol. 71, pp. 1008-1010, 1997.
- [3] M. Schmitz, R. Brauer, and O. Bryngdahl, "Gratings in the resonance domain as polarizing beam splitters," *Opt. Lett.*, Vol. 20 pp. 1830-1832, 1995.
- [4] X. T. Lia, A. Natansohn, and P. Rochon, "Photoinduced liquid crystal alignment based on a surface relief grating in an assembled cell," *Appl. Phys. Lett.*, Vol. 74, pp. 3791-3793, 1999.
- [5] C. J. Barrett, A. Natansohn, and P. L. Rochon, "Photoinscription of channel waveguides and grating couplers in azobenzene polymer thin films," *Proc. SPIE*, Vol. 3006, pp. 441-449, 1997.
- [6] Z. Sekkat, and W. Knoll eds., *Photoreactive organic thin films*, Academic Press: USA, 2002.
- [7] P. Lefin, C. Fiorini, and J.-M. Nunzi, "Anisotropy of the photoinduced translation diffusion of azo-dyes," *Opt. Mater.*, Vol. 9, pp. 323-328, 1998.
- [8] S. Bian, J. Williams, D. Kim, L. Li, S. Balasubramanian, J. Kumar, and S. Tripathy, "Photoinduced surface deformations on

- azobenzene polymer films," *J. Appl. Phys.*, Vol. 86, pp. 4498-4508, 1999.
- [9] C. Barrett, P. Rochon, and A. Natansohn, "Model of laser-driven mass transport in thin films of dye-functionalized polymers," *J. Chem. Phys.*, Vol. 109, pp. 1505-1516, 1998.
- [10] T. Pedersen, P. Johansen, N. Holme, P. Ramanujam, and S. Hvilsted, "Mean-field theory of photoinduced formation of surface reliefs in side-chain azobenzene polymers," *Phys. Rev. Lett.*, Vol. 80, pp. 89-92, 1998.
- [11] J. Kumar, L. Li, X. Jiang, D. Kim, T. Lee, and S. Tripathy, "Gradient force: the mechanism for surface relief grating formation in azobenzene functionalized polymers," *Appl. Phys. Lett.*, Vol. 72, pp. 2096-2098, 1998.
- [12] D.Y. Kim, Lian Li, X.L. Jiang, V. Shivshankar, J. Kumar, and S.K. Tripathy, "Polarized laser induced holographic surface relief gratings on polymer films," *Macromolecules*, Vol. 28, 8835-8839, 1995.
- [13] M. Ho, C. Barrett, J. Paterson, M. Esteghamatian, A. Natansohn, and P. Rochon, "Synthesis and Optical Properties of Poly {(4-nitrophenyl)- [3- [N- [2- (methacryloyloxy) ethyl]- carbazolyl]] diazene}," *Macromolecules*, Vol. 29, pp. 4613-4618, 1996.
- [14] I. Naydenova, T. Petrova, N. Tomova, V. Dragostinova, L. Nikolova, and T. Todorov, "Holographic investigations on side-chain azobenzene copolymers of acrylic type," *Polym. Prep.*, Vol. 39, 342-343, 1998.
- [15] N. C. R. Holme, L. Nikolova, P. S. Ramanujam, and S. Hvilsted, "An analysis of the anisotropic and topographic gratings in a side-chain liquid crystalline azobenzene polyester," *Appl. Phys. Lett.*, Vol. 70, pp. 1518-1520, 1997.
- [16] B. Darracq, F. Chaput, K. Lahlil, Y.Lévy, and J.-P. Boilot, "Photo-inscription of Surface Relief Gratings on Azo-Hybrid Gels," *Adv. Mater.*, Vol. 10, pp. 1133-1136, 1998.
- [17] T. S. Lee, D. Y. Kim, X. L. Jiang, L. Li, J. Kumar, and S. K. Tripathy, "Photoinduced surface relief gratings in high-Tg main-chain azoaromatic polymer films," *J. Polym. Sci. A*, Vol. 36, pp. 283-289, 1998.
- [18] M. Sukwattanasinitt, X. Wang, L. Li, X. L. Jiang, J. Kumar, S. K. Tripathy, and D. J. Sandman, "Functionalizable self-assembling polydiacetylenes and their optical properties," *Chem. Mater.*, Vol. 10, pp. 27-29, 1998.
- [19] C. Hubert, C. Fiorini, I. Maurin, J.-M. Nunzi, and P. Raimond, "Spontaneous patterning of hexagonal in an azo-polymer using light-controlled mass transport," *Adv. Mater.*, Vol. 14, pp. 729-732, 2002.
- [20] S. Ahmadi Kandjani, R. Barille, S. Dabos-Seignon, J.-M. Nunzi, E. Ortyl, and S. Kucharski, "Multistate polarization addressing using a single beam in an azo polymer film," *Opt. Lett.*, Vol. 30, pp. 1986-1988, 2005.
- [21] E. Ortyl and S. Kucharski, "Refractive index modulation in polymeric photochromic films," *Centr. Eur. J. Chem.*, Vol. 1, pp. 137-159, 2003.
- [22] E. Ortyl, R. Janik, and S. Kucharski, "Methacrylate polymers with photochromic side chains containing heterocyclic sulphonamide substituted azobenzene," *Eur. Polym. J.*, Vol. 38, pp. 1871-1879, 2002.
- [23] M. S. Ho, A. Natansohn, and P. Rochon, "Azo Polymers for Reversible Optical Storage. 7. The Effect of the Size of the Photochromic Groups," *Macromolecules*, Vol. 28, pp. 6124-6127, 1995.
- [24] H. A. Schneider, "Flexibility and phase transitions of polymers," *J. Appl. Polym. Science*, Vol. 88, pp. 1590-1599, 2003.
- [25] T. Matsui, S. Yamamoto, M. Ozaki, K. Yoshino, and F. Kajzar, "Relaxation kinetics of photoinduced surface relief grating on azopolymer films," *J. Appl. Phys.*, Vol. 92, pp. 6959-6965, 2002.

THIS PAGE IS INTENTIONALLY LEFT BLANK.